

Structure and Electrical Resistance of the Passivating ZnSe Layer on Ge

Volodymyr Maslov (✉ vpmaslov@ukr.net)

V E Lashkaryov Institute of Semiconductor Physics NAS of Ukraine: Institut fiziki napivprovidnikov imeni V E Laskar'ova Nacional'na akademiya nauk Ukraini <https://orcid.org/0000-0001-7795-6156>

Artem Fedorenko

V E Lashkaryov Institute of Semiconductor Physics NAS of Ukraine: Institut fiziki napivprovidnikov imeni V E Laskar'ova Nacional'na akademiya nauk Ukraini

Vasyl Kladko

V E Lashkaryov Institute of Semiconductor Physics NAS of Ukraine: Institut fiziki napivprovidnikov imeni V E Laskar'ova Nacional'na akademiya nauk Ukraini

Alexandr Gudymenko

V E Lashkaryov Institute of Semiconductor Physics National Academy of Sciences of Ukraine: Institut fiziki napivprovidnikov imeni V E Laskar'ova Nacional'na akademiya nauk Ukraini

Nataliia Zashchepkina

National Technical University of Ukraine Igor Sikorsky Kyiv Polytechnic Institute: Nacional'nij tehnicnij universitet Ukraini Kiivs'kij politehnicnij institut imeni Igora Sikors'kogo

Kostiantin Bozhko

National Technical University of Ukraine Igor Sikorsky Kyiv Polytechnic Institute: Nacional'nij tehnicnij universitet Ukraini Kiivs'kij politehnicnij institut imeni Igora Sikors'kogo

Nano Express

Keywords: Ge, photodetector, ZnSe layer, GeSe and GeSe₂ phases, X-ray phase investigation, electrical resistance, elastic contact

Posted Date: April 19th, 2021

DOI: <https://doi.org/10.21203/rs.3.rs-415311/v1>

License:  This work is licensed under a Creative Commons Attribution 4.0 International License.

[Read Full License](#)

Abstract

When creating a passivating ZnSe layer on Ge, which is used in *p-i-n* Ge photodetector, we found two additional phases GeSe and GeSe₂ that does not contradict with their state diagram. The above phases can have an essential effect on performances of the passivating layer. Therefore, to study the electrical resistance of this layer we prepared model samples of layers containing the GeSe and GeSe₂ with the thickness 0.5...1.8 μm and area 1 cm². To measure the electrical resistance of these layers, we used elastic contacts. The performed measurements have shown that Se layers on Ge have an intermediate resistance between that of ZnSe on Ge and pure Ge, and, therefore, the effect of additional phases practically does not worsen the passivating properties of the ZnSe layer on Ge.

Introduction

In laser ranging and fiber-optic communication, near infrared (NIR) spectral range is usually used, because of this range comprises the so-called “transparency windows” for their operation media (atmosphere, glass, silica...). It is this range that is suitable for wide application of germanium (Ge) photodetectors [2 – 5].

Various materials are now used for passivation of surfaces in Ge photodetectors [6]. As it is offered in [7], the protective film of photo-converter can be made of zirconium dioxide (ZrO₂) or fianite – single crystal of cubic solid solutions based on zirconium dioxide mixed with stabilizing oxides of yttrium (Y₂O₃), scandium (Sc₂O₃) or lanthanides. This technical solution enables to improve photoelectric parameters, to provide stability, reliability and life span to eliminate excess noise in Ge photodiodes of a large area. In its coefficient of thermal expansion, a SiO₂ film differs two-fold as compared with that for Ge and creates thermal stress after vacuum depositing and cooling. Besides, there can take place creation of an additional layer from Ge oxide, which worsens dielectric properties of the SiO₂ layer.

In multilayer Ge photoconverters [8], the Si₃N₄ layer is used as the passivating one. This material possesses a low coefficient of thermal expansion and has many positive properties, namely: mechanical strength, chemical inertness and high dielectric permittivity. But this way has its deficiencies: technological difficulties in manufacturing and necessity to use very expensive equipment. The coefficient of thermal expansion for this material ($3.4 \cdot 10^{-6} \text{ K}^{-1}$) approaches to that of germanium ($6.1 \cdot 10^{-6} \text{ K}^{-1}$), but differs by the value $3 \cdot 10^{-6} \text{ K}^{-1}$, which makes it impossible to deposit protective layers of the necessary thickness close to 1 μm. The layers of this thickness are characterized by increasing the internal stresses, when being used in Ge photoconverters. The internal stresses reduce the operating life and reliability of photoconverters.

As a passivating layer for fast Ge *p-i-n* photodetectors, there used was the zinc selenide (ZnSe) one [9]. This material has a high transparency in the NIR range, therefore it can be deposited both onto front and

side surfaces to protect the *p-i-n* junction. It should enable to provide passivation and improve its performances, including reliability.

Decreasing the surface currents is reached owing to wide forbidden gap inherent to ZnSe 2.7 eV, as compared to that of intrinsic Ge 0.67 eV. One of the advantages for applying ZnSe as the protective and passivating layer for germanium photoconverters is its value of thermal expansion coefficient $6.1 \cdot 10^{-6} \text{ K}^{-1}$ that is very close to that of germanium – $7.1 \cdot 10^{-6} \text{ K}^{-1}$. It is also important that ZnSe has no oxygen in its composition, therefore it does not oxidize germanium during the technological process of deposition, which provides absence of an additional layer of germanium oxides.

The optimum values of ZnSe passivating layer thickness lie within the range 0.8...1.5 μm . The detectors with this passivating layer demonstrate high stability of their parameters for more than two years.

To perform X-ray and electrical measurements, we prepared model samples of plates with the area 1 cm^2 from germanium and glass covered with ZnSe layers (thermally deposited in vacuum) of various thickness within the range 0.8...1.5 μm . Besides, there prepared were the same plates with Se layers to analyze the created structures and their properties.

The aim of this work was to study the structure and electrical resistance of the layers consisting of ZnSe, GeSe phases as well as GeSe₂ on Ge surface.

Methods Of Investigations

X-ray phase analysis of the samples was performed using the diffractometer Philips X'Pert PRO – MRD. CuK_{α1} radiation ($\lambda = 0.15406 \text{ nm}$) was used in these experiments. The voltage of 45 kV was applied to the tube anode, the current was 40 mA. Diffractograms were taken both in the symmetrical and grazing geometries with various slopes of the sample surface relatively to the direction of X-ray beam. It provided lowering the strong peak from the germanium substrate in orientation (111). The qualitative phase analysis of diffractograms was carried out using the database ICDD.

Studying the electrical resistance of surface layers was performed using the method of elastic contacts [10], which has the following important advantages as compared to the four-probe method:

- large area of the contact zone, which provides a low current density and, respectively, absence of Joule heating;
- low pressure onto the semiconductor surface, which enables to minimize distraction of this surface;
- applying the contacts with the maximum possible area covering the whole sample enables to avoid the influence of geometrical errors.

The theory of electrical contacts is represented in detail in [11]. The elastic contacts are of special interest. Investigations of them started from the work [12]. Composite materials, including those from

nanomaterials, are widely researched for applying in electronic facilities as elastic contacting elements [13 – 16].

Application of the elastic contacts based on rubber having the anisotropic electrical conductivity is now widely used in liquid-crystal indicators (Liquid Cristal Displays – LCD). We used the contacts manufactured by the firm Fujitsu (Japan).

One of the promising fields of using this method is pulsed voltammetry [17] with its distinctive feature – duration of measuring pulses reaches here 100 ms or higher, while the interval between pulse trains exceeds 1 s. The pulsed methods for measuring the resistance of thin films as well as semiconductor surface layers find their wide application in recent years [18, 19].

Shortening the time for measurements by using short measuring pulses (single or serial with a high off-duty ratio) enables to minimize heating the thin films. The pulse methods allow changing both the amplitude and temporal parameters of pulses: their duration, repetition frequency and off-duty ratio. This enables to optimize the measuring methods for every type of surfaces – various kinds of metals and semiconductors, as well as composites and nanomaterials.

The structural scheme of stand for pulsed measurements of the surface resistance is shown in Fig. 1.

The measurements were performed in the following regime: pulses of the amplitude 4 to 10 V, frequency 160 kHz and off-duty ratio 3 to 8 from the generator enter the voltage divider that consists of the resistor 1...140 kOhm and the studied sample with applied elastic contacts. The signals from generator and the sample (midpoint of the voltage divider) enter the digital oscillograph (channels 1 and 2). The obtained values are used to calculate the surface resistance of the studied sample.

Before measurements, it was experimentally found that the zone of reliable contact begins from the pressure 20 kPa. After 3-fold increasing it, the resistance value decreases only by one third. Therefore, when measuring the resistance of fragile materials, it is sufficient to use the pressure 20...30 kPa that is two orders less than that used in the four-probe method.

The measurements of electrical resistance we carried out using the pulsed method on the 2101th reading at the scale of digital oscillograph. The instant voltage value at the generator output was kept the same. The pulses were taken from the generator based on the timer NE555, the amplitude of pulses was 4.84 ± 0.04 V. The pressure applied to elastic contacts was 20 kPa.

Topology of the sample surface was studied using the atomic-force microscope.

Results Of Measurements And Discussion

First of all, the prepared samples of Ge plates with the ZnSe layer were studied using the atomic-force microscope (Fig. 2). It was necessary to determine quality of the ZnSe layer obtained after deposition.

The roughness of the sample was $R_a = 12.7$ nm, $R_z = 25$ nm. These values were typical for all the samples.

The diffractograms of model samples Nos 1 to 4 (Fig. 3) contain the peaks of cubical phase inherent to polycrystalline ZnSe with the lattice parameter $a = 5.6687\text{\AA}$ [20].

When the diffractograms were taken in the grazing geometry with the angle of X-ray incidence 15° , an additional diffraction peak appears at the angle 25.92° (blue curve in Fig. 4). The appearance of a diffracted beam within the definite narrow interval of angles of incidence onto the sample is usually inherent to textured phases. It is the most probable that this reflection (201) belongs to the hexagonal textured phase GeSe with the following parameters: $a = 8.7\text{\AA}$, $c = 8.32\text{\AA}$ [21]. The diffractogram obtained for the angle of incidence 10° contains an additional diffraction peak at 28.76° (red curve in Fig. 4). It is the most probable that it corresponds to the reflection (112) belonging to the tetragonal textured phase of GeSe_2 with the parameters: $a = 5.7307\text{\AA}$, $c = 9.691\text{\AA}$ [22]. It is worth to note that the axes of GeSe and GeSe_2 phases textures practically coincide with the direction of the plane (111) inherent to the Ge substrate and are declined from it by only 5...8 degrees.

When studying the samples with deposited pure Se layers, we observed creation of textured phases GeSe and GeSe_2 (Fig. 5). Availability of the increased diffusive background is indicative of the presence of an amorphous phase. It is noteworthy that creation of the Se crystalline phase was not observed. It was logical to assume that the textured phases GeSe and GeSe_2 were created at the hetero-boundary between pure Ge and amorphous Se layer.

In what follows, we adduce the results of measuring the electrical resistance of some samples. The example of oscillogram for the sample No 4 with the thickness of ZnSe layer $0.9\text{ }\mu\text{m}$ is shown in Fig. 6. The values of specific resistance for the samples Nos 4 and 3_77 are summarized in Table 1.

Table 1. Specific resistances of ZnSe and Se layers deposited onto Ge substrates.

Parameter	ZnSe	ZnSe	Se
Layer thickness, μm	0.9	1.5	1.5
Specific resistance, $\text{k}\Omega/\square$	8.81 ± 0.2	13.29 ± 0.2	10.1 ± 0.3

The resistance of the samples ZnSe on Ge with the phases GeSe and GeSe_2 is higher than that of the samples Se on Ge with the same additional phases. Therefore, one can make the conclusion that the properties of ZnSe layer as the isolating one are more preferable for Ge substrate. The same relationship was observed between specific resistances in the samples with ZnSe and Se layers on glass. Therefore, the influence of GeSe and GeSe_2 phases on isolating properties of passivating coatings can be considered as insignificant.

Conclusions

To ascertain the effect of additional phases GeSe and GeSe₂ on the passivating properties of ZnSe coating in Ge photodiodes, it has been developed the method based on using the elastic contacts. The studies were carried out on model samples with an area of 1 cm² and a thickness of ZnSe and Se films of 0.5-1.8 μm, containing the indicated phases, on Ge substrates and control samples of films of the same thickness on glass. X-ray studies have shown the presence of textured GeSe and GeSe₂ phases in samples with both ZnSe films and Se films. The electrical resistance of ZnSe samples on a Ge substrate is higher in comparison with the resistance of Se samples on a Ge substrate. Taking into account these results for the electrical resistance in aggregate with the data of small differences in lattice parameters and thermal expansion coefficients of Ge and ZnSe layer (with the thickness 0.8...1.5 μm), which provides the absence of internal stresses, passivation of Ge photodiodes with ZnSe seems to be expedient.

References

1. Golovynskyi S., Golovynska I., Stepanova L., Datsenko O., Liu Liwei, Qu Junle, Ohulchanskyy Tymish, Optical windows for head tissues in near and short-wave infrared regions: approaching transcranial light applications / Journal of Biophotonics, 2018, <https://doi.org/10.1002/jbio.201800141>
2. Luca Alloatti. Closed-loop silicon germanium photodetector apparatus and other semiconductor devices including curved-shape silicone germanium structures // patent US 2017/0040487 A1, publ. 09.02.2017
3. Thomas Wetteland Baer-Jones, Yi Zhang, Michael J. Hochberg, Ari Novak Germanium metal-contact-free near-IR photodetector// Patent US 2017/0104116 A1, publ. 13.04.2017.
4. M. Shank, J.J. Ellis-Monaghan, J.S. Orcutt Germanium photodetector with SOI doping source // Patent US 2017/0162743 A1, publ. 08.01.2017.
5. Novack, Y. Liu, Y. Zang Lateral Ge/Si avalanche photodetector // International patent WO 2017/023301 A1, publ. 09.02.2017.
6. Suppression of dark current in germanium-tin on silicon p-i-n photodiode by a silicon surface passivation technique / Yuan Dong, Wei Wang, Dian Lei, Xiao Gong, Qian Zhou, Shuh Ying Lee, Wan Khai Loke, Soon-Fatt Yoon, Eng Soon Tok, Gengchiao Liang, and Yee-Chia Yeo / OPTICS EXPRESS, 2015 | Vol. 23, No. 14.
7. .A. Kosukhina, Yu.V. Lobikov, M.S. Sidorov, M.A. Trishenkov, T.A. Khromova, I.V. Chinaryova. Germanium planar photodiode // Patent of Russian Federation No 87 569 from 10.10.2009 (in Russian).
8. V.M.Andreyev, N.D. Il'inskaya, N.A. Kalyuzhnyi, V.M. Lantratov, A.V. Malevskaya, S.A. Mintairov. The way to manufacture the multilayer photo-converters // Patent of Russian Federation No 2 368 038 from 09.2009, Bulletin No 26 (in Russian).
9. Maslov V.P., Sukach A.V., Tet`orkin V.V. et al. Peculiarities of manufacturing, electrical and photoelectrical properties of diffusion Ge *p-i-n* photodiodes// Optoelektronika i poluprovodnikovaya

- tekhnika. 2018, No 53, p. 188– 198 ([n Ukrainian]).
10. Ryssel H., Rugel. Ion implantation. – Wiley, Chichester, 1986. – 478 p.
 11. Braunovich M., Konchits V., Myshkin N. Electrical Contacts. Fundamentals, Applications and Technology. – CRC Press. – Boca Raton, Fl., 2007. – 660 p.
 12. Tamai T. Electrical Properties of Conductive Elastomer as Electrical Contact Material //IEEE Transactions on Components, Hybrids and Manufacturing Technology, Volume: 5 , Issue: 1 , Mar 1982. – Pages: 56 – 61.
 13. Shenogin S., Ferguson L., Roy A. The effect of contact resistance on electrical conductivity in filled elastomer materials //Polymer, Volume 198, 3 June 2020
<https://doi.org/10.1016/j.polymer.2020.122502>Get rightsandcontent
 14. Rogers, J.A.; Someya, T.; Huang, Y. Materials and mechanics for stretchable electronics //Science 2010, 327, Pages:1603–1607.
 15. Kim, D.H.; Rogers, J.H. Stretchable electronics: Materials strategies and devices //Advanced Materials, 2008, 20, Pages:4887–4892.
 16. Saleem, A.; Frommann, L.; Soever, A. Fabrication of extrinsically conductivesilic on erubbers with high elasticity and analysis of the ir mechanical and electrical characteristics //Polymers,2010, 2, Pages:200–210.
 17. Molina A., González J. Pulse Voltammetry in Physical Electrochemistry and Electroanalysis: Theory and Applications. – Springer. – 2016. – 671 p.
 18. Saotome, S. Oi, and H. Kaneko, “Development of contactless measuring instrument for sheet resistance by means of pulse voltage excitation,” IEEJ Trans. Sens. Micromachines, vol. 133, pp.52-53, February 2013.
 19. Deen M.J., Pascal F. (2017) Electrical Characterization of Semiconductor Materials and Devices. In: Kasap S., Capper P. (eds) Springer Handbook of Electronic and Photonic Materials. Springer Handbooks. Springer, Cham. https://doi.org/10.1007/978-3-319-48933-9_20
 20. Yeh, C., Lu, Z.W., Froyen, S., Zunger, A. Phys. Status Solidi 25 93 (1967)
 21. Karbanov et al. Inorg. Mater. (Engl. Transl.) 6 104 (1970)
 22. Grande, T., Ishii, M., Akaishi, M., Aasland, J. Solid State Chem. 145 167 (1999)

Figures

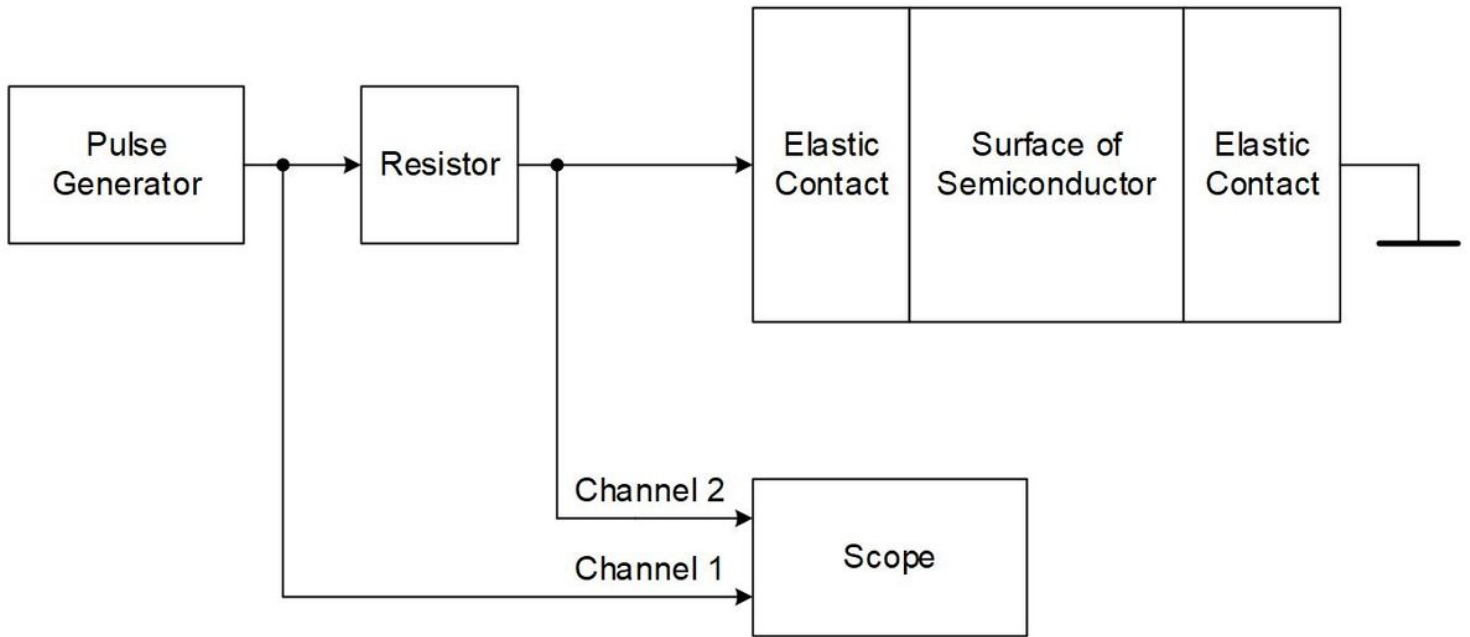


Figure 1

Stand for pulsed measurements of the surface resistance with using the elastic contacts.

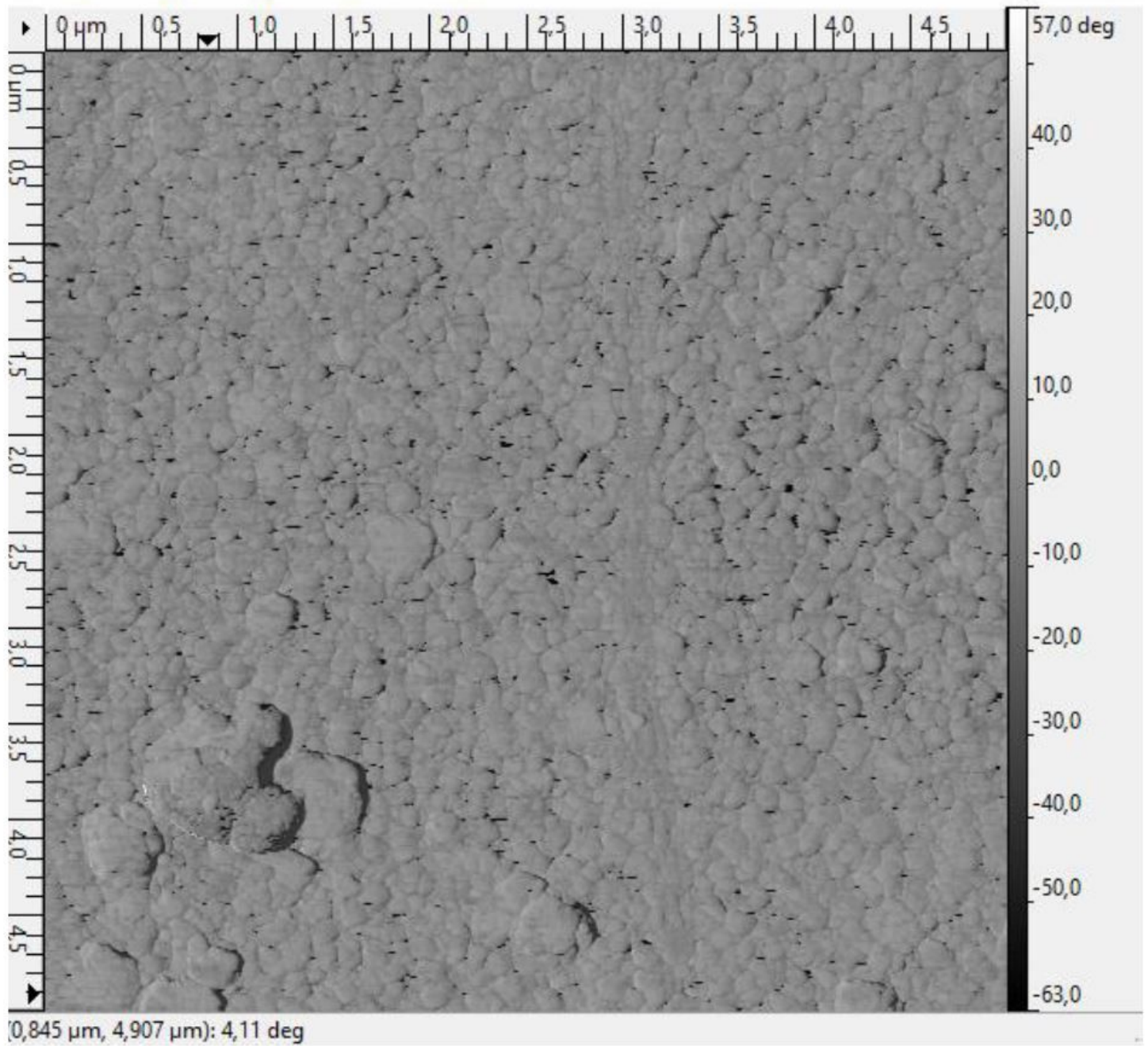


Figure 2

Topology of the ZnSe layer surface after deposition onto germanium.

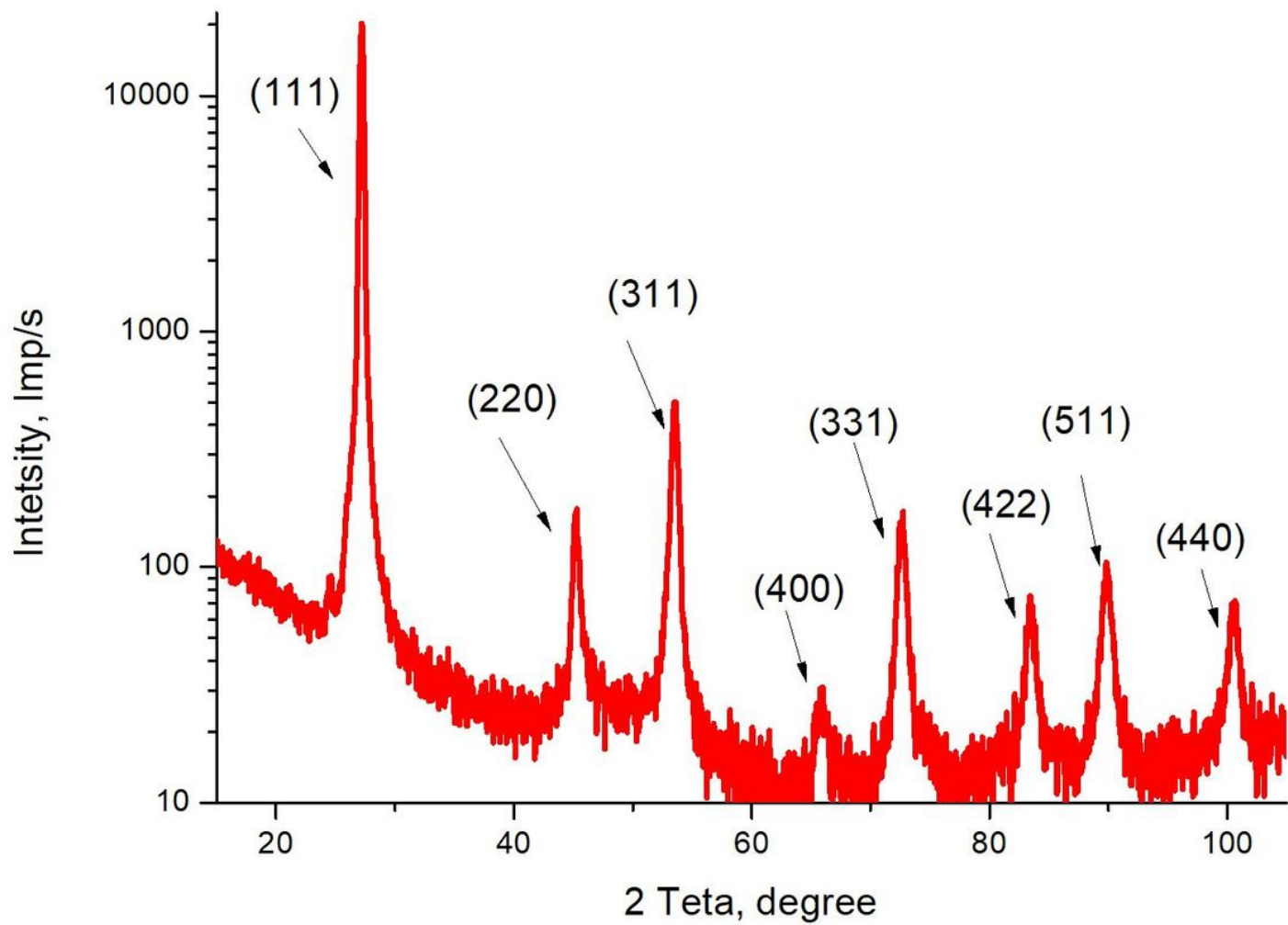


Figure 3

Diffraction pattern of the sample No 2 (ZnSe layer on Ge, the thickness 0.6 μm)

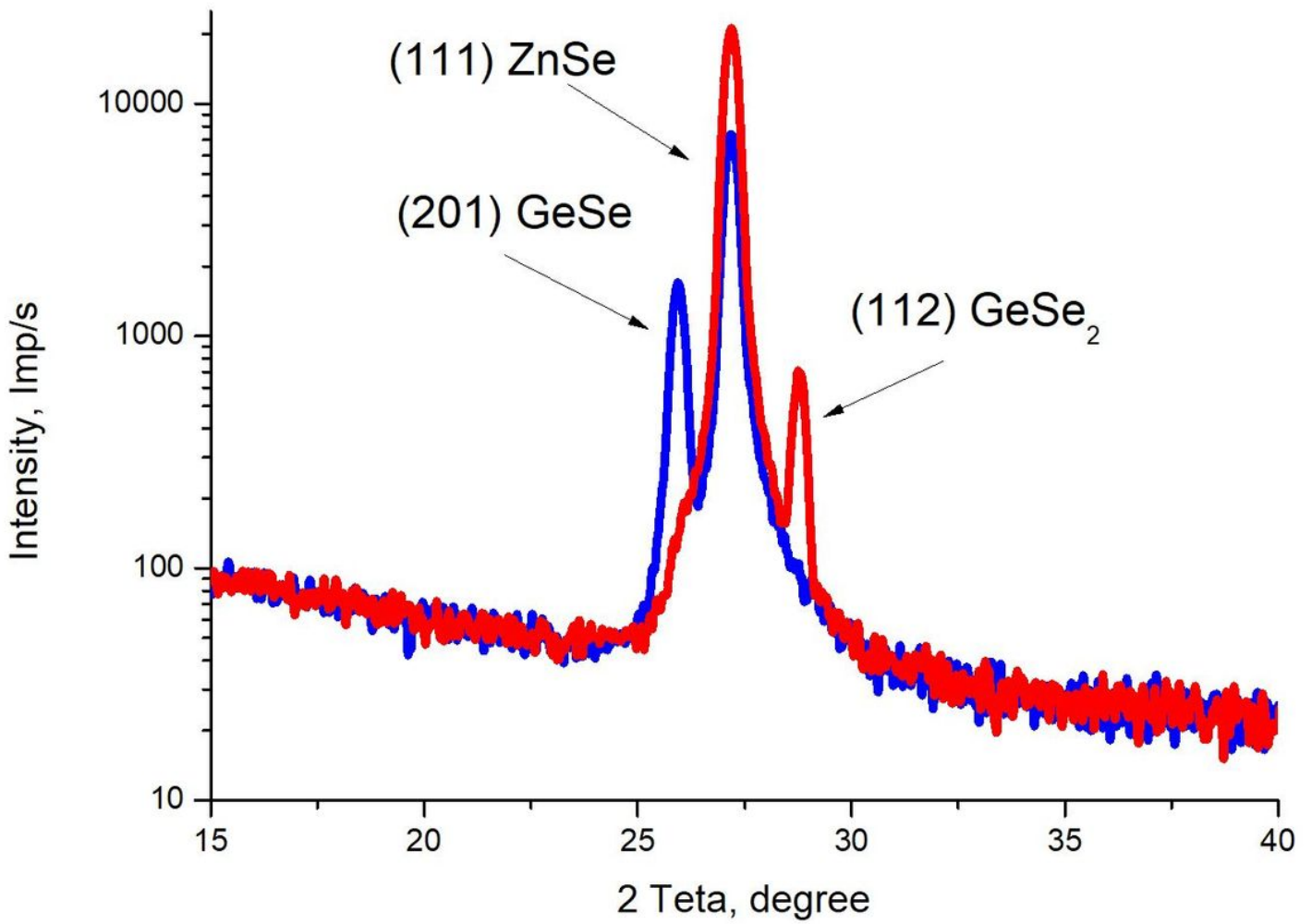


Figure 4

Diffractogram of the sample No 2 (ZnSe layer on Ge). The blue curve corresponds to the angle of X-ray incidence 150, the red curve – to 100.

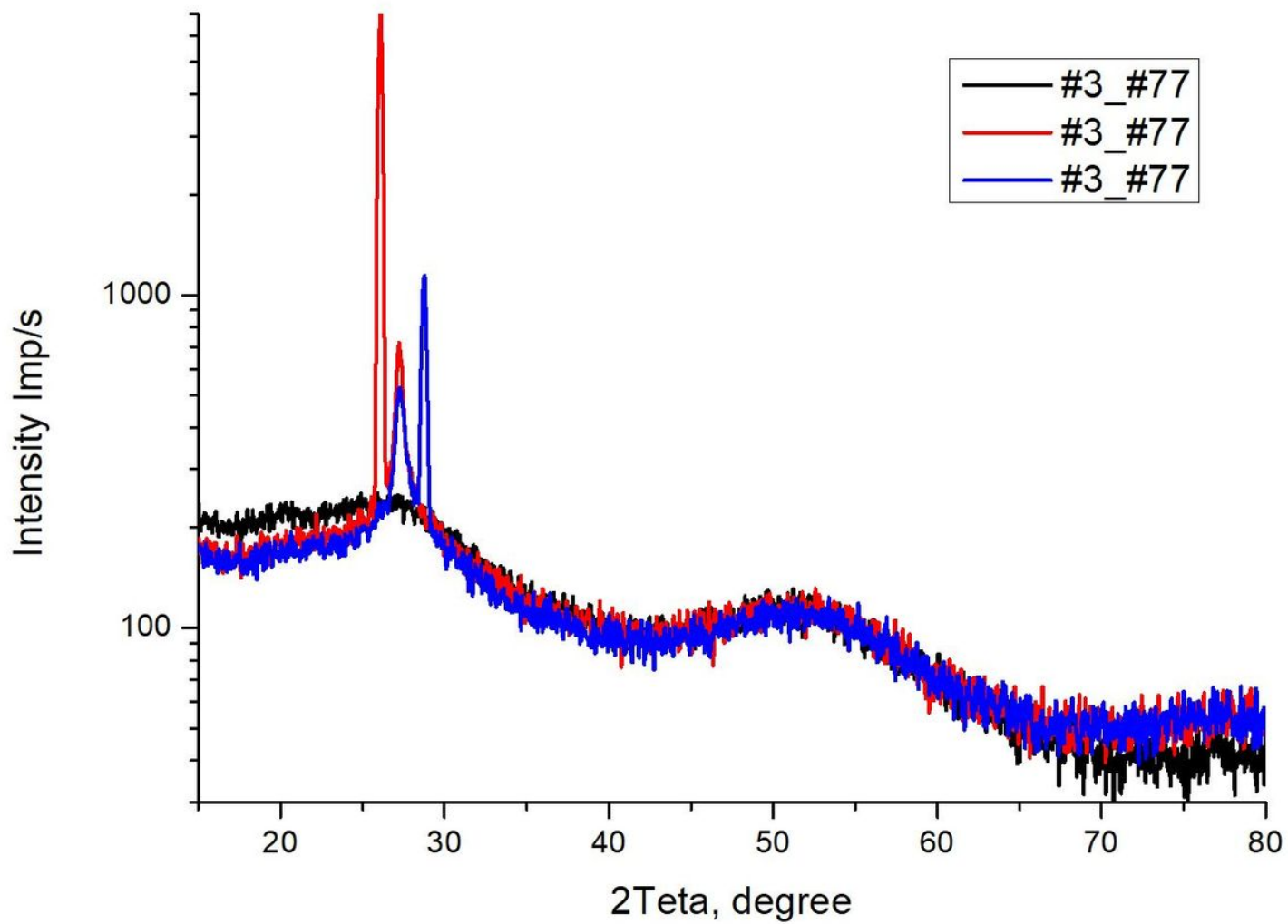


Figure 5

Diffractogram of the sample No 3_77.

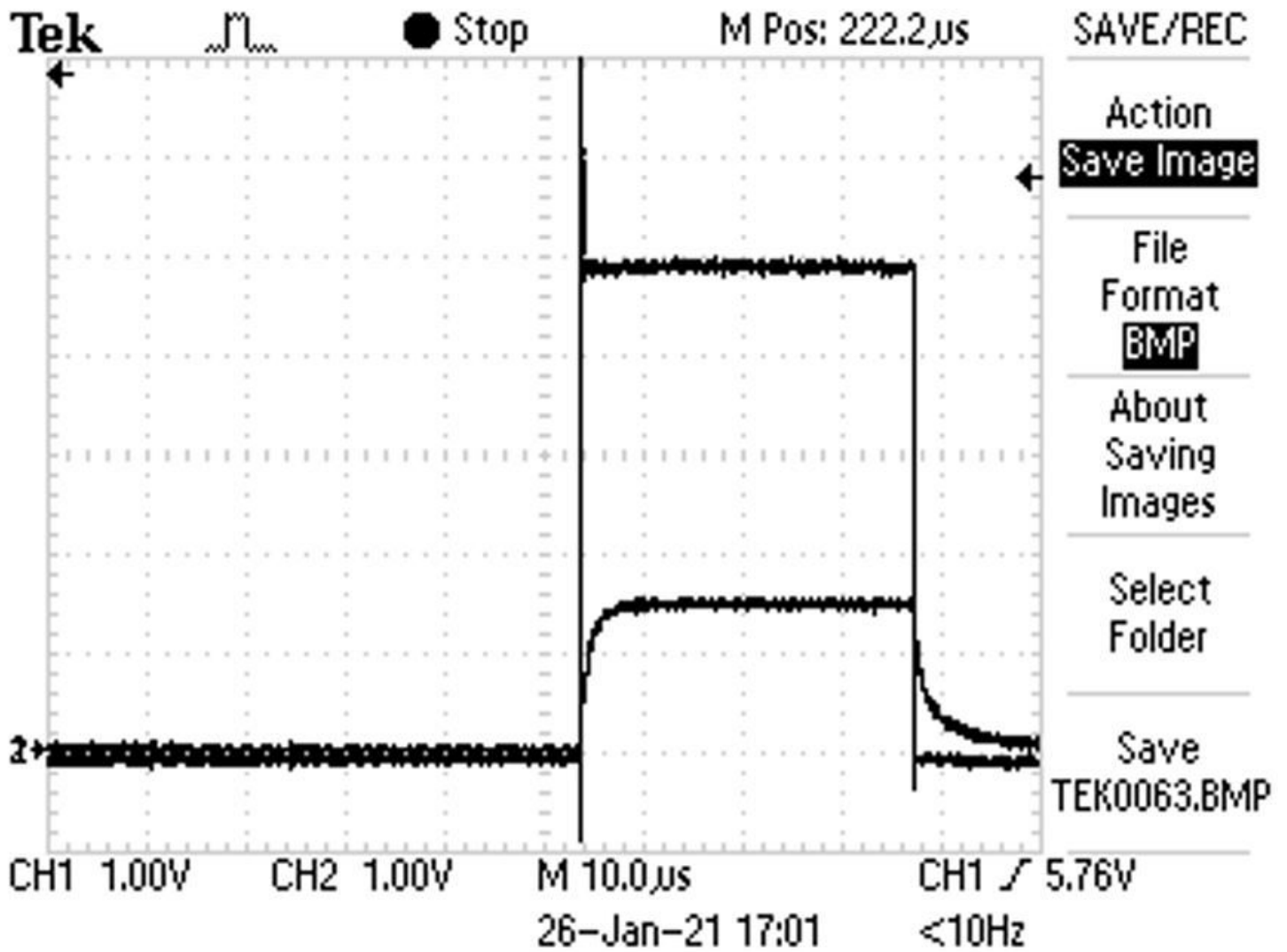


Figure 6

Oscilloscope of the sample No 4 (ZnSe layer on Ge, thickness 0.9 μ m).